THE ASTRONOMICAL JOURNAL, 118:2409–2423, 1999 November

A WIYN LITHIUM SURVEY FOR YOUNG STARS IN THE λ ORIONIS STAR-FORMING REGION

CHRISTOPHER J. DOLAN AND ROBERT D. MATHIEU
Department of Astronomy, University of Wisconsin–Madison, 475 North Charter Street, Madison, WI 53706; dolan@astro.wisc.edu; mathieu@astro.wisc.edu
Received 1999 April 15; accepted 1999 July 20

ABSTRACT

We have found 72 pre–main-sequence (PMS) stars near the center of the λ Orionis star-forming region by spectroscopically testing a magnitude-limited sample for the presence of lithium λ6708 absorption, a diagnostic of youth. All of these stars show large lithium equivalent widths and radial velocities consistent with Orion membership, but only two were discovered previously via Hα or X-ray surveys. Comparison with PMS evolutionary tracks show that the low-mass star formation did not begin prior to the initiation of high-mass star formation 5–7 Myr ago. However, the subsequent detailed star formation history is model dependent. Baraffe et al. isochrones imply that high- and low-mass stars began to form together 5–7 Myr ago, with the low-mass stellar formation ceasing abruptly 1 Myr ago. On the other hand, D'Antona & Mazzitelli isochrones indicate a narrow spread of PMS ages, which suggests a burst of low-mass star formation 1–2 Myr ago. Furthermore, kinematic arguments require that the parent molecular cloud gravitationally bound the stars together until recently, but at present the requisite gas mass is not visible. This leads us to conjecture that both the high- and low-mass stars were in a tightly bound cluster until a supernova blast about 1 Myr ago disrupted the parent cloud. This supernova also impacted on the PMS formation process by either (1) ceasing formation through removal of the gas supply or (2) triggering star births via cloud compression, depending on choice of stellar evolution models. Finally, we find that despite their youth, only four of the 72 PMS stars have T Tauri–like Hα emission, suggesting the absence of accretion disks. We conjecture that this may be the result of photoevaporation of the disks while the low-mass stars were in much closer proximity to the OB stars prior to becoming gravitationally unbound.

Key words: stars: formation — stars: pre–main-sequence

1. INTRODUCTION

With 11 OB stars[1] centered in a cleared ring of molecular clouds littered with low-mass pre–main-sequence (PMS) stars, the λ Orionis star-forming region is a superb laboratory for studying a young stellar population. These OB stars have shredded their parent cloud (Maddalena & Morris 1987, hereafter MM87; Lang & Masheder 1998), creating an ionized region with low obscuration ($E_{B-V} = 0.12$ for λ Ori itself; Diplas & Savage 1994) surrounded by dense gas, as shown in Figure 1. Duerr, Imhoff, & Lada (1982, hereafter DIL82) performed a complete objective-prism Hα survey of the region to find 83 emission objects, many of which are likely to be classical T Tauri stars (CTTSs). Their star counts show an enhanced surface density near the inner edges of the dark clouds B30 and B35 (Gomez & Lada 1998), just inside the ionization front. More recently, the *ROSAT* All Sky Survey (RASS) has uncovered a population of about 80 hard X-ray sources (Sterzik et al. 1995) that may be associated with young members of the association. Follow-up identification and spectroscopy of roughly 60 stars (Alcalá et al. 1996; Magazzù et al. 1997) revealed that 35 of these X-ray sources have substantial lithium λ6708 absorption, a diagnostic of youth. As in other star-forming regions, some of these X-ray/lithium stars have been cross-referenced with the CTTSs, but many more are weak-lined T Tauri stars (WTTSs) that have not been previously identified as young. However, the flux limit of the RASS allows only the brightest X-ray PMS stars to be detectable at the distance of λ Ori (roughly 15% of them, based on numbers from Briceño et al. 1997). Additionally, Wolk (1996) found that as many as 50% of WTTSs in a star-forming region may be X-ray quiet, suggesting that X-ray surveys may be strongly incomplete.

From the spatial distribution of detected sources, it appears that the low- and high-mass stars are quite segregated. To paraphrase Gomez & Lada (1998), there are two possible explanations for this: (1) the lack of low-mass PMS stars near the OB stars is physical or (2) there are PMS stars throughout the entire star-forming region, but many do not have strong Hα emission or bright X-rays. The former case may imply that the mass distribution of stars formed in the immediate vicinity of the OB stars (i.e., the local initial mass function [IMF]) is skewed toward higher mass. The latter suggests that there may be a substantial population of young, low-mass stars not yet identified in the vicinity of the OB stars.

To distinguish between these two scenarios, one needs to survey the vicinity of the OB stars with an unbiased diagnostic of youth. For very young late-type stars, a good diagnostic is lithium λ6708 absorption. Lithium works as a youth diagnostic because it has a fusion ignition temperature lower than hydrogen. Consequently, lithium is depleted during the convective PMS stages of late-type stars. However, the need for high spectral resolution to unambiguously detect the lithium line has made it an impractical tool for large surveys with conventional spectrographs. The advent of fiber-optic, multiobject spectrographs now offers us a new tool to search for PMS stars. The multiplexing advantage of these instruments

[1] Murdin & Penston (1977, hereafter MP77), identified 12 OB stars, but one of them, HD 245370, is an F8 mislabeled as a B8

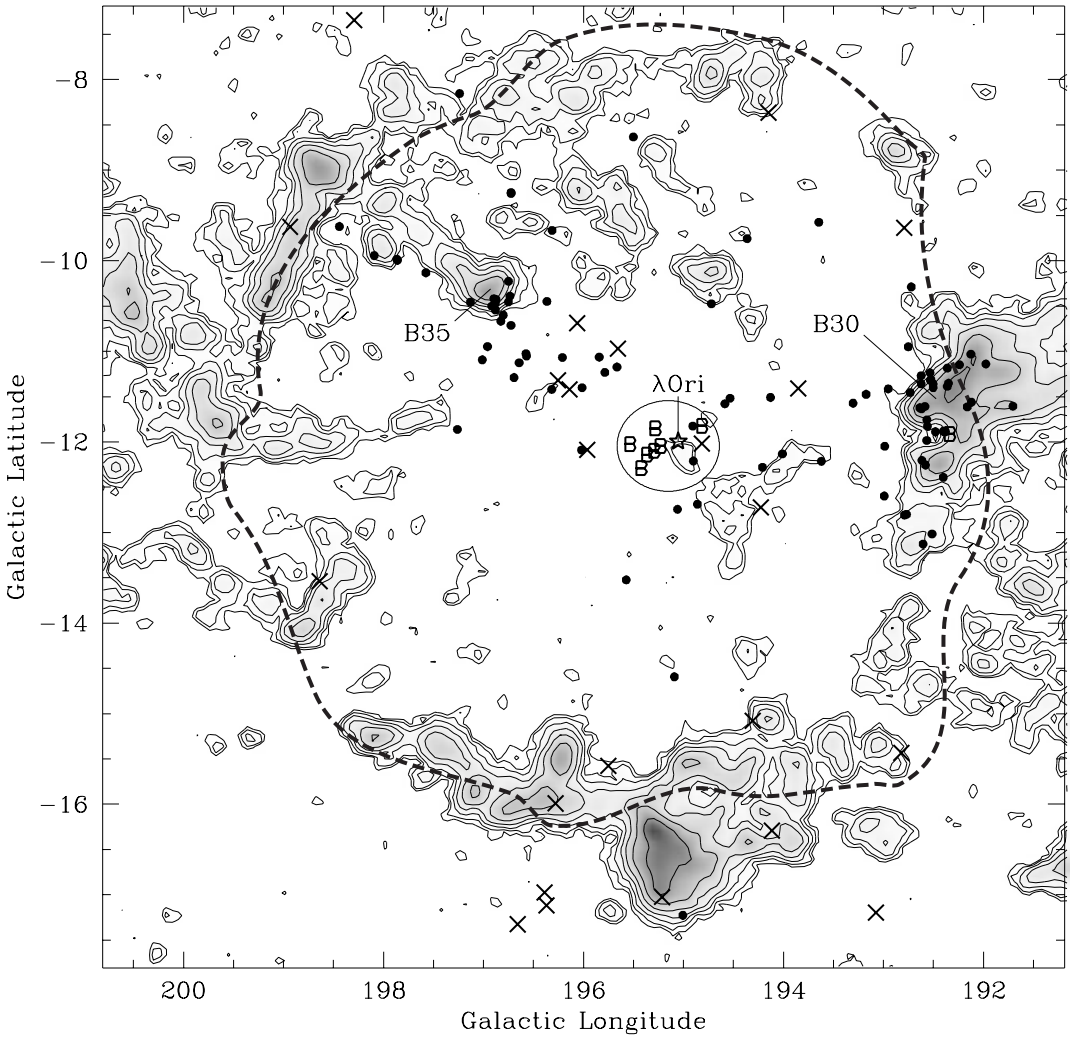

FIG. 1.—Compilation of literature data. The gray scale and contours depict a CO $J = 1 \rightarrow 0$ map adapted from Lang & Masheder (1998). The dashed outline is the border of the ionization front, as inferred from the Swarthmore Hα Survey (J. Gaustad 1998, private communication). The solid dots are Hα sources cataloged by DIL82. The crosses are *ROSAT*-detected PMS stars from Alcalá et al. (1996) and Magazzù et al. (1997). The "B" symbols mark the B stars (MP77), while the circle around them marks the scope of observations presented in this paper.

allows us to forego the Hα or X-ray survey that is typically needed to sift through a sample of stars before time-consuming high-resolution spectroscopic work commences.

In this paper, we report the results of a survey for low-mass stars with strong lithium absorption near λ Ori using the WIYN[2] Multi-Object Spectrograph (MOS). We find that this survey technique is very effective, revealing many more PMS stars than were previously known from other surveys. With a sample of PMS stars in hand, we attempt to deduce the connection between the low- and high-mass stars by examining the age, mass, and spatial and kinematic distributions of the PMS stars in relation to the OB stars, using models of PMS evolution. These analyses, with additional input from *Hipparcos* proper-motion data for some of the OB stars and Hα emission measurements for the PMS stars, suggest a star formation history that may include prolonged gravitational binding by dense gas and a recent (∼1 Myr) disruptive event that dispersed the gas and left an imprint on the PMS star formation rate.

2. DATA

In 1997 September, G. Jacoby kindly obtained *VRI* photometric images for us centered on λ Ori and including the neighboring B stars marked in Figure 1 (J2000, R.A. $5^h35^m26^s$, decl. $+9°53'00''$) with the 8K × 8K Mosaic imager on the KPNO 0.9 m telescope. The 1° field of the Mosaic on the 0.9 m telescope is perfectly matched to the 1° field of MOS on WIYN, but the imager was equipped with engineering-grade CCD chips, which have numerous large defects. We reduced the images with the 1997 October prototype version of IRAF-MSCRED package, but because of the CCD defects we chose to forego the usual step of identifying stars with a routine such as DAOFIND. Instead, we registered our images to the astrometric system of the USNO-A1.0 catalog (Monet et al. 1996) and ran IRAF-PHOT on all of the 4200 objects brighter than $R = 17$ in the USNO catalog that lay within our 1° field. We chose this method because (1) we wanted to use the high-quality USNO astrometry as input to MOS and (2) we wished to

[2] The WIYN Observatory is a joint facility of the University of Wisconsin-Madison, Indiana University, Yale University, and the National Optical Astronomy Observatories.

avoid the step of distinguishing point sources among defects on our images.

We followed up this photometry with images on a subset of the field as an external check on the photometry. In 1998 March, H. Bond took V and I images for us in three 23 arcmin^2 fields with the 2K imager on the KPNO 0.9 m telescope, and in 1998 April, F. Vrba took V and R images in the same three fields with the 1K (12 arcmin^2) imager on the USNO 1 m telescope. Comparison with the high-quality VRI photometry from these images demonstrated that our Mosaic data had RMS precisions of 0.050 (V), 0.045 (R), and 0.041 (I) mag (1 σ). We also found and corrected small systematic offsets in the Mosaic photometry. The resulting R versus $R-I$ color-magnitude diagram (CMD) is shown in Figure 2. Because the central λ Ori region is nearly transparent, most of the stars shown are likely field stars.

We then used the Mosaic photometry to select stars we wished to observe spectroscopically. Our photometric selection criteria are shown as a solid line in Figure 2. One of our prime objectives is to study the chronology of star formation relative to the 2–6 Myr old OB stars (MP77), so we chose photometric limits that would include low-mass stars much older and much younger than the OB stars. Thus, we selected stars which lay above a 30 Myr isochrone in the CMD, assuming a distance of 400 pc (MP77). In addition, we set a faint limit of $R = 16$ by the ability of the spectrograph to acquire adequate signal in a 2 hr exposure. With these criteria, as well as $12 < R < 16$, $R-I < 3$, and $V-R < 3$ (the latter two criteria to cull stars with photometry corrupted by CCD defects), we found 550 candidate stars to observe spectroscopically. In the end, we had a few extra fibers, so we included a handful of red stars with $16 < R < 16.5$ in the sample, as marked by the dashed addendum in Figure 2.

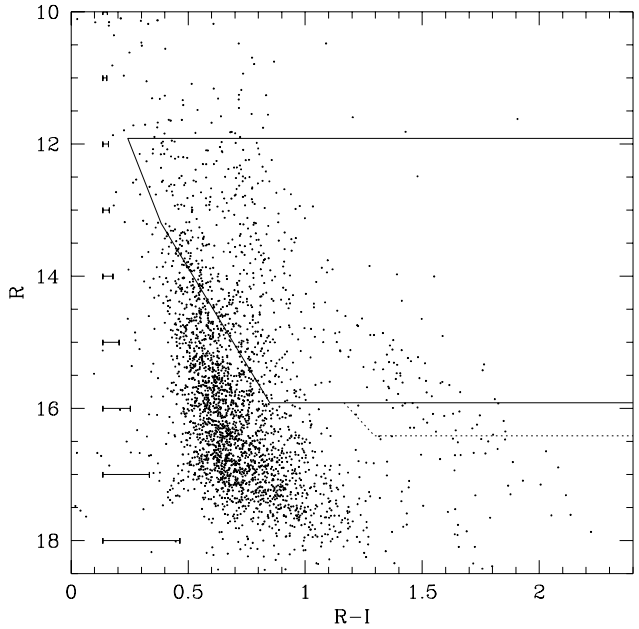

FIG. 2.—Color-magnitude diagram showing 3049 stars in the 1° field surrounding the OB stars. The error bars show the average random error in $R-I$ for a given magnitude. The solid line delimits the region from which we selected sources for spectroscopic follow-up. We observed 95% of the selected sources within the primary region (*solid line*) and 29% of the sources in the addendum below it (*dashed line*).

Prior to this work, there were three known young stars in our field besides the OB stars: two from the DIL82 Hα survey (DIL 52 and DIL 54) and one from Alcalá et al. (1996) via the RASS (RXJ 0534.6+1007). The former two are in our sample, while the latter was too bright for our survey.

Our spectrograph setup used the echelle grating centered at 6640 Å to obtain spectra with a resolution of 0.6 Å. This setup allowed us to observe Li I λ6708 and Hα, as well as a sample of metal lines near 6450 Å for precise radial-velocity computation. Seven WIYN pointings in 1997 November and December and 1998 February allowed us to collect 612 spectra of 537 stars, representing 95% of our selected stars. The typical signal-to-noise ratio (S/N) per pixel for these spectra ranged from 25 to 40. Each pointing included at least seven fibers placed in random positions for measurement of the sky brightness. For each pointing, we obtained one dome flat and two Th-Ar spectra for fiber-to-fiber throughput and wavelength calibration. These calibrations allowed us to subtract sky and compute radial velocities.

We extracted and reduced the spectra using IRAF-HYDRA. We identified lithium λ6708 absorption lines by eye and measured equivalent widths, W_λ(Li), by fitting a Gaussian profile to the line in the continuum-divided spectra. Our spectral resolution and continuum S/N allows us to detect a lithium line with an equivalent width of 0.1 Å with about 5 σ confidence for a narrow-lined star. A rotating star with $v \sin i$ greater than our instrumental profile of 25 km s^{-1} would have a lower confidence level at this limit. We detected lithium λ6708 absorption in 128 stars, approximately a quarter of our sample. Of these, 72 show "strong" lithium absorption indicative of youth, as discussed in detail in § 3.

We used the cross-correlation package IRAF-FXCOR to compute radial velocities relative to either a solar (sky) spectrum or a high S/N spectrum of HD 95735 (M2 V) obtained during our 1997 December run.[3] Internally, we find that for the 69 stars with two or more measurements, the mode of the velocity dispersion for each star is 1.2 km s^{-1}, which is a good estimate of our measurement precision. This dispersion is comparable to our typical precision with this instrument, measured over the past 3 yr. We do not have an external check for these velocities, but we have found the Sun to be an adequate zero-point calibrator in previous WIYN-MOS runs, resulting in velocities accurate to 0.5 km s^{-1}, compared with external velocity measurements.

Finally, we used IRAF-SPLOT to measure the equivalent width of Hα lines in the spectra for which we detected lithium absorption. Because the Hα line was often irregular in shape, we computed this equivalent width by directly integrating under the line, unlike the fitting procedure we used for our lithium measurements.

The data for the 72 stars with strong lithium are presented in Table 1. The star identifier comes from the USNO-

[3] We detected a systematic offset of ~3–4 km s^{-1} in our M2 V template velocities, so in a June 1998 WIYN observing run at 5100 Å, we calibrated HD 95735 against the M0.5 III radial-velocity standard star HD 146051. We found a velocity for HD 95735 of −81.2 km s^{-1}, 3.8 km s^{-1} larger than the literature velocity of −85.0 km s^{-1} (Evans 1967). Adopting the −81.2 km s^{-1} value, we found that the M2 V template velocities match well the G2 V–template velocities.

TABLE 1

PRE–MAIN-SEQUENCE STELLAR DATA

ID	USNO ID[a]	R.A.	Decl.	V	$V-R$	$R-I$	W_λ(Li)[b] (Å)	W_λ(Hα)[b] (Å)	V_r	N
1.....	728134	5 33 47.25	09 55 38.75	14.37	0.85	0.99	0.56	2.51	22.44	2
2.....	728971	5 33 49.89	09 50 38.34	16.62	1.12	1.39	0.47	24.95	24.03	2
3.....	729523	5 33 51.75	09 38 21.88	14.83	0.87	1.12	0.44	3.18	21.27	1
4.....	731002	5 33 56.38	09 53 57.25	16.23	1.50	1.55	0.33	4.41[c]	2.40[d]	1
							0.31		55.26	
5.....	732776	5 34 02.03	09 41 06.38	13.50	0.73	0.76	0.46	0.06	28.98	1
6[e].....	733727	5 34 05.00	09 57 04.14	16.77	1.14	1.44	0.43	72.64	29.09	1
7.....	733876	5 34 05.58	09 42 46.75	13.01	0.67	0.68	0.42	−0.12	25.48	1
8.....	736498	5 34 13.71	09 29 20.17	13.68	0.72	0.65	0.41	−0.09	27.73	1
9.....	742440	5 34 32.77	09 59 29.81	14.60	0.88	0.78	0.40	0.74	24.64	2
10	743185	5 34 35.18	09 27 49.69	17.21	1.31	1.59	0.51	5.97	29.06	1
11	743340	5 34 35.64	09 59 43.63	16.95	1.28	1.57	0.63	3.63	26.61	1
12	743524	5 34 36.25	09 53 44.57	16.55	1.50	1.43	0.66	6.07	28.87	1
13	743996	5 34 37.81	09 31 53.31	15.44	0.98	0.92	0.53	1.29	27.91	1
14	744438	5 34 39.23	09 52 55.33	15.18	0.82	1.06	0.57	2.28	25.66	1
15	744604	5 34 39.73	09 41 46.19	16.10	1.02	1.13	0.49	1.07	27.31	1
16	744630	5 34 39.82	10 06 22.24	16.74	1.31	1.45	0.61	5.45	24.12	1
17	745513	5 34 42.49	10 11 54.09	13.72	0.86	0.80	0.47	0.25	24.70	1
18	747051	5 34 47.27	10 02 42.86	15.02	1.48	0.94	0.52	2.64	23.97	1
19	747437	5 34 48.49	09 57 15.93	15.97	1.04	1.20	0.56	2.07	27.53	1
20	747629	5 34 49.04	09 58 02.27	16.66	1.26	1.57	0.61	3.45	19.18	1
21	747947	5 34 49.95	09 41 01.28	14.80	0.94	0.96	0.50	1.73	23.65	1
22	748126	5 34 50.47	09 51 47.81	15.95	1.07	1.08	0.54	2.37	24.37	1
23	749161	5 34 53.75	09 26 57.51	15.92	1.05	1.05	0.53	2.04	26.68	1
24	753261	5 35 06.06	10 00 19.57	12.85	0.57	0.53	0.30	−1.07	29.15	1
25	753571	5 35 06.97	09 48 57.93	15.52	0.96	1.09	0.54	1.47	23.55	1
26	754046	5 35 08.36	09 42 54.15	13.02	0.64	0.62	0.35	−0.39	24.96	1
27	754264	5 35 09.05	09 27 00.20	16.52	1.20	1.49	0.59	3.64	27.62	1
28	754424	5 35 09.56	09 32 09.74	14.05	0.61	0.84	0.47	−0.35	27.94	1
29	756225	5 35 15.16	10 01 06.82	16.93	1.23	1.63	0.54	4.13	30.52	1
30	756871	5 35 17.18	09 51 11.97	16.59	1.00	1.46	0.61	1.00	27.56	1
31	757028	5 35 17.69	09 23 44.88	13.77	0.69	0.65	0.42	−0.01	24.13	1
32	757263	5 35 18.44	10 02 38.44	17.65	1.40	1.56	0.42	5.50	28.54	1
33	757765	5 35 19.95	10 02 36.94	16.99	1.61	1.41	0.52	10.92	23.33	1
34	758276	5 35 21.51	09 44 10.68	16.85	1.07	1.41	0.49	2.64	30.66	1
35	758493	5 35 22.22	09 52 27.80	15.71	0.88	1.28	0.55	1.68	24.11	1
36	759575	5 35 25.40	10 08 38.42	16.50	1.30	1.47	0.54	30.00	27.44	1
37	760729	5 35 29.00	09 35 21.33	15.65	1.26	0.87	0.43	0.08	27.07	2
38	761244	5 35 30.49	09 50 34.20	17.47	1.46	1.88	0.74	8.20	18.71	1
39	762676	5 35 34.83	10 00 35.71	15.99	1.05	1.18	0.36	3.14	24.55	2
40	762976	5 35 35.76	09 44 35.77	17.23	1.16	1.53	0.55	3.63	27.05	1
41	764209	5 35 39.50	09 50 33.21	17.00	1.31	1.64	0.64	3.90	27.73	1
42	767164	5 35 48.64	10 19 12.18	16.85	1.09	1.41	0.58	2.94	28.69	1
43	767384	5 35 49.38	09 38 18.43	17.62	2.23	1.43	0.57	2.60	26.17	1
44	768060	5 35 51.34	09 55 11.21	15.85	1.13	1.30	0.54	4.39	24.16	1
45	769053	5 35 54.35	10 04 23.32	13.05	0.66	0.66	0.46[c]	−0.12[c]	68.49[d]	1
									−20.54	
46	769433	5 35 55.45	09 56 31.01	14.42	0.97	0.89	0.55	3.35	17.62	1
47	769507	5 35 55.69	09 50 53.34	17.66	1.39	1.90	0.57	8.65	28.89	1
48	769553	5 35 55.86	09 56 21.93	17.11	1.24	1.45	0.58	8.61	28.21	1
49	769966	5 35 57.10	09 46 52.91	16.91	1.29	1.54	0.55	3.59	28.93	1
50	770155	5 35 57.69	09 47 34.35	15.62	1.02	1.19	0.47	1.95	24.54	1
51	770231	5 35 57.93	09 54 33.58	14.66	0.96	1.00	0.55[c]	1.65[c]	8.78[d]	1
									61.01	
52	770781	5 35 59.57	09 27 24.48	13.98	0.55	0.61	0.25	−0.36	21.96	1
53	771864	5 36 02.90	09 42 07.80	15.29	0.92	1.00	0.52	3.62	23.15	3
54	773330	5 36 07.13	10 09 47.60	16.85	1.16	1.47	0.61	4.22	28.68	1
55	774117	5 36 09.32	09 47 02.82	16.57	1.20	1.51	0.62	6.83	27.82	1
56	776595	5 36 16.63	09 50 48.49	15.51	1.03	1.14	0.59	2.02	19.47	2
57	777292	5 36 18.59	09 45 09.09	14.02	1.26	0.65	0.39	−0.15	28.33	1
58	777454	5 36 19.06	10 03 50.84	15.03	0.96	0.99	0.55	1.45	26.40	1
59	777880	5 36 20.24	09 44 02.24	15.73	1.04	1.23	0.53	3.95	24.93	2
60	777982	5 36 20.53	09 52 18.94	15.35	1.09	0.96	0.49	0.80	25.43	1
61	779981	5 36 26.34	09 51 14.11	16.71	1.25	1.30	0.56	4.23	27.96	1

TABLE 1—*Continued*

ID	USNO ID[a]	R.A.	Decl.	V	$V-R$	$R-I$	W_λ(Li)[b] (Å)	W_λ(Hα)[b] (Å)	V_r	N
62.....	780883	5 36 28.93	09 54 27.15	16.64	1.15	1.35	0.61	4.05	28.62	1
63.....	783945	5 36 38.06	09 40 51.01	13.84	0.83	0.80	0.54	4.76	25.80	1
64.....	784150	5 36 38.63	09 35 05.73	16.27	1.14	1.42	0.45	2.52	28.05	2
65.....	786976	5 36 47.12	10 05 51.89	16.09	1.01	1.19	0.58	2.67	25.98	1
66.....	788718	5 36 52.09	09 34 02.93	13.31	0.71	0.76	0.55	1.00	15.98	1
67.....	788939	5 36 52.66	09 52 56.58	16.79	1.06	1.67	0.66	4.88	29.98	1
68.....	789081	5 36 53.09	09 41 55.77	13.81	0.71	0.70	0.44	−0.04	26.95	1
69.....	789663	5 36 54.88	09 50 25.10	15.65	1.03	1.04	0.51	0.49	26.35	1
70.....	790569	5 36 57.52	09 53 25.88	16.49	1.28	1.20	0.58	0.90	24.60	1
71.....	794902	5 37 10.19	09 55 26.99	16.82	1.15	1.39	0.52	19.33	26.68	2
72.....	800238	5 37 25.37	09 53 44.96	16.45	0.94	1.81	0.64	6.38	27.52	1

NOTE.—Units of right ascension are hours, minutes, and seconds, and units of declination are degrees, arcminutes, and arcseconds.

[a] From the USNO-A1.0 catalog, Monet et al. 1996; each name is in the format 0975-01 <nnnnnn>.

[b] Positive W_λ(Li) values indicate *absorption*. Positive W_λ(Hα) values indicate *emission*.

[c] W_λ measured from the combined light of both components.

[d] Double-lined spectrum.

[e] DIL 52.

[f] DIL 54.

A1.0 catalog, as do the coordinates. The next three columns are V, $V-R$, and $R-I$ photometry measured from our Mosaic images. The following three columns present our spectroscopic data: lithium equivalent width, Hα equivalent width, and stellar radial velocity. The last column is the number of spectra we have for the star in question. Three stars (stars 4, 45, and 51) show double-line correlation spectra, so the two components are listed on separate lines. For one of these three (star 4), two distinct lithium lines were visible, so we list the observed equivalent width for each line.

3. LOW-MASS STARS

Our discussion of the λ Ori star-forming region focuses separately on the low- and high-mass stars, which we discuss in turn.

3.1. *Membership and Youth*

In our spectra, we have two independent diagnostics of membership in the star-forming region: lithium and radial velocities. These two membership diagnostics agree well, as seen in Figure 3, which compares lithium equivalent width to radial velocity for the 128 stars with detected lithium. These data show a distinct bimodality between the "weak-lithium" stars, which show a broad spread of velocities, and the "strong-lithium" stars, which are confined to a very narrow range of velocities. The former category has 56 stars with $W_\lambda(\mathrm{Li}) \leq 0.12$ Å, while the latter contains 72 stars with $W_\lambda(\mathrm{Li}) \geq 0.25$ Å. Note that we have marked our three double-line spectra with an open circle for each of the two components in Figure 3.

The narrow spread of velocities in the strong-lithium sample suggests that these stars are all part of the same association. Excluding the three double-lined stars, the mean heliocentric velocity of the strong-lithium stars is 24.3 km s^{-1}, with a dispersion of 2.8 km s^{-1} (or 2.6 km s^{-1} correcting for our 1.2 km s^{-1} measurement error). $V_{\mathrm{Helio}} =$ 24.3 km s^{-1} corresponds to $V_{\mathrm{LSR}} = 9.1$ km s^{-1}, which is consistent with the gas velocity of the nearby B30 and B35 clouds ($V_{\mathrm{LSR}} = 10.2$, 11.5 km s^{-1}; Maddalena et al. 1986). Curiously, models by MM87 and Lang & Masheder (1998) of the molecular gas as a nearly face-on expanding ring predict that the LSR gas velocity at the center, where these stars are located, should be 6.0 and 3.8 km s^{-1}, respectively.

3.2. *Age of the Stars*

Large lithium equivalent width is a diagnostic of stellar youth. For a given $R-I$ value, stars with higher lithium equivalent widths than stars in a zero-age main-sequence (ZAMS) cluster are very likely to be PMS. We make such a demonstration in Figure 4 by comparing our stars with lithium detections to those in the Pleiades, a canonical ZAMS cluster. Rather than showing the Pleiades stars themselves, we display an envelope (adapted from

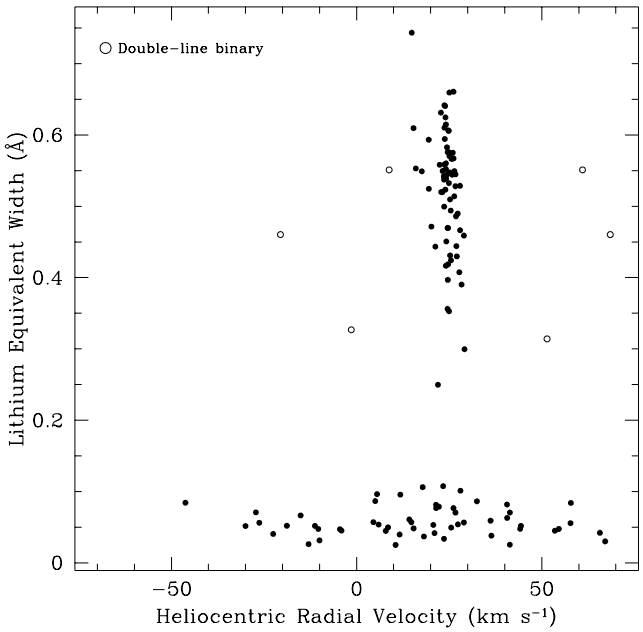

FIG. 3.—Discrimination between field stars and young λ Ori members. Displayed are the 128 stars for which we have detected lithium λ6707 absorption. 72 stars have distinctly stronger lithium absorption. These same stars have a mean radial velocity of 24.3 km s^{-1} and a velocity dispersion of only 2.6 km s^{-1}, consistent with the velocities of the B30 and B35 clouds. We conclude the lithium-rich stars are all members of the λ Ori association.

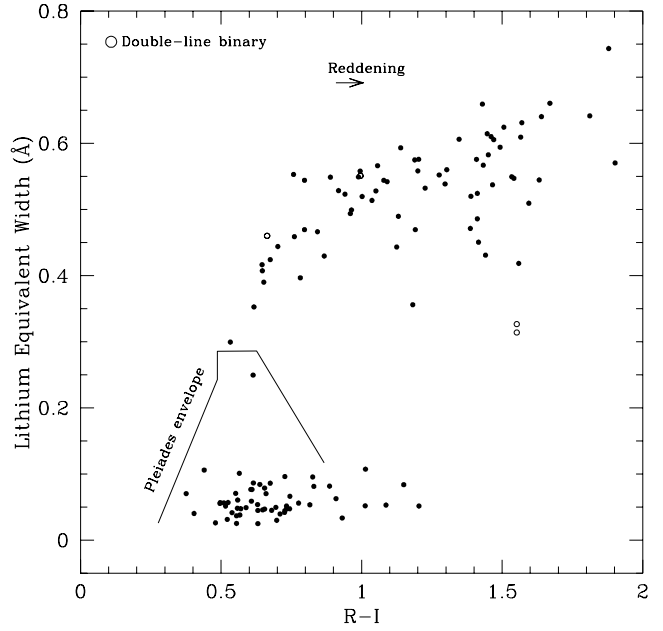

FIG. 4.—Lithium equivalent width of all the stars from Fig. 3 compared with that of the Pleiades, the canonical ZAMS cluster. The line represents the upper envelope of lithium for Pleiades stars, adapted from Neuhaüser et al. (1997) and reddened by 0.097 mag. Our stars have substantially more lithium than the Pleiades stars, with absorption strengths similar to very young T Tauri stars.

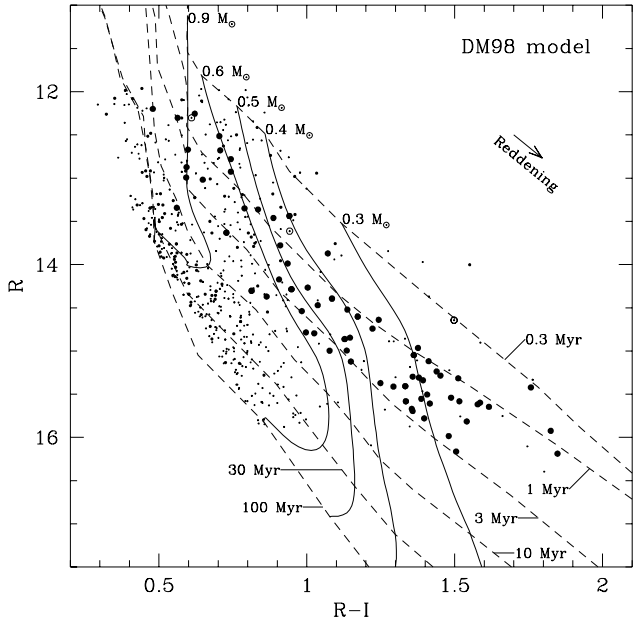

FIG. 5.—CMD annotated with our spectroscopic results. The dots mark the stars we observed spectroscopically. The largest dots mark stars with lithium equivalent widths greater than 0.2 Å. The medium-sized dots indicate stars with lithium detections, but with W_λ(Li) < 0.2 Å. The smallest dots mark lithium nondetections. The three open circles mark double-line binaries. The dashed lines are DM98 isochrones with solar metallicity and intermediate deuterium abundance. The solid lines are the evolution tracks for the same models. The reddening vector ($E_{R-I} = 0.097$ and $A_R = 0.27$) is adapted from the Diplas & Savage (1994) measurement of $E_{B-V} = 0.12$ for λ Ori assuming $R_V = 3.1$.

Neuhaüser et al. 1997) defining the maximum lithium equivalent widths detected in Pleiades members. In this figure, we reddened the Pleiades envelope by 0.097 mag to match the value of $E_{B-V} = 0.12$ measured for λ Ori.

Our strong-lithium stars are well above the youth threshold defined by the Pleiades envelope, from which we argue that they are PMS members of the association. At the same time the weak-lithium sample lies below the Pleiades envelope, consistent with our conclusion that these are field stars.

While lithium is a valuable tool to qualitatively determine youth, we rely on comparison with PMS evolutionary models to make quantitative measures of stellar ages. Here we transform the models into the color-magnitude plane to compare them with our data.

In Figures 5 and 6, we have plotted the stars that we observed with WIYN. In Figure 5 we mark the stars with dot sizes according to the three categories in which they fall: strong lithium, weak lithium, or nondetection of lithium. The majority of the weak-lithium stars lie near the blue edge of our selection box. The strong-lithium stars form a well-defined locus extending far to the red of most of the field population, consistent with our suggestion that these are PMS stars in the association. In Figure 6, we disregard the weak-lithium stars and plot the strong-lithium stars with a dot size proportional to W_λ(Li). There is a clear trend for the faint, red stars to have the strongest lithium absorption lines, as expected from stellar atmosphere theory.

On each CMD we have displayed PMS isochrones for ages between 0.3 and 10 Myr, which includes the span of ages of the B stars. For reference, we have also displayed 30 and 100 Myr isochrones. The latter shows the location of the ZAMS, while the former approximately defines the limit of the oldest stars in which we could have detected lithium at 400 pc, given our photometric selection criteria.

For Figure 5, the isochrones we display are adapted from D'Antona & Mazzitelli (1997 and 1998, hereafter collectively DM98), choosing a metallicity of $Z = 0.02$ and a deuterium abundance of 2×10^{-5}. In Figure 6 we show Baraffe et al. (1998; hereafter BCAH98) solar metallicity iso-

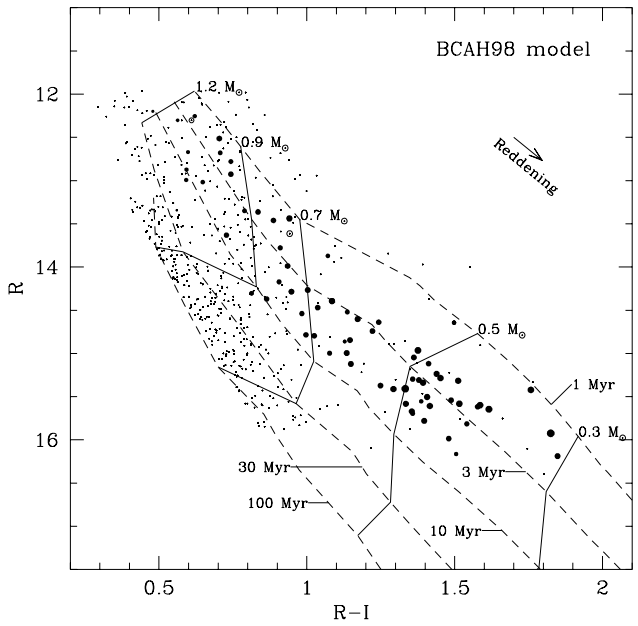

FIG. 6.—Similar to Fig. 5 except that the isochrones and evolution tracks are from the solar metallicity models of BCAH98. In this figure, only stars with strong lithium absorption are highlighted, these being association members. For these stars, the dot size is proportional to W_λ(Li).

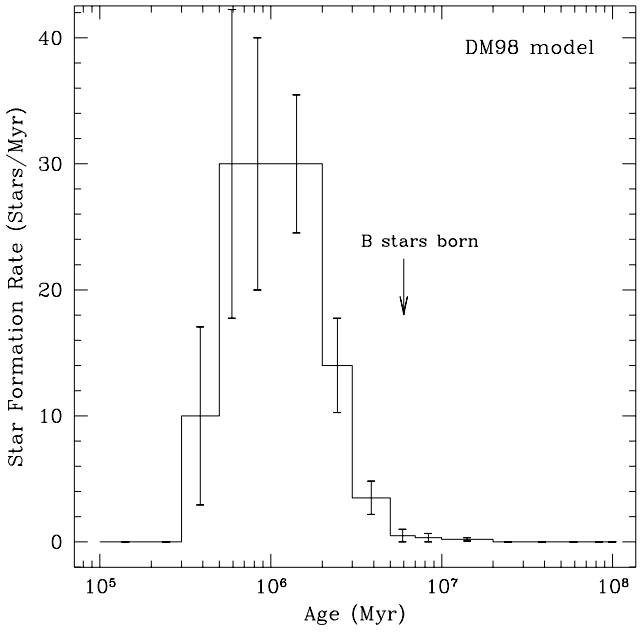

FIG. 7.—Star formation rate vs. time for our strong-lithium sample measured by comparison with the DM98 isochrones shown in Fig. 5. This plot indicates that the majority of the PMS stars are much younger than the massive stars and that the birth rate peaked recently.

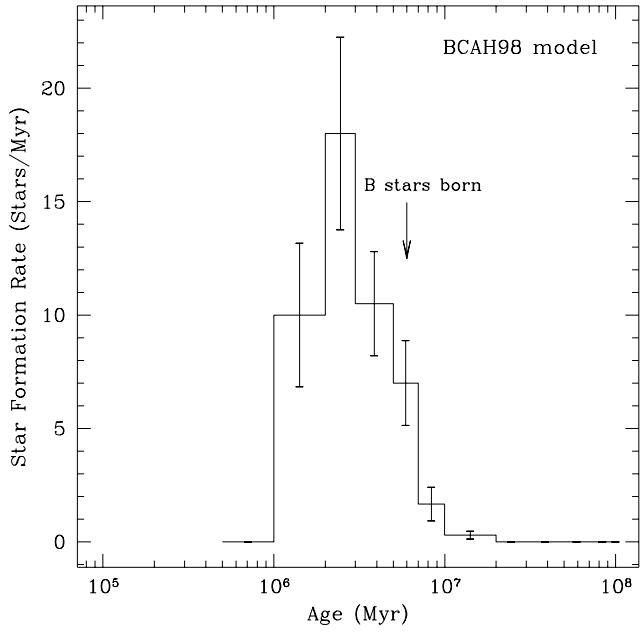

FIG. 8.—Identical to Fig. 7 except that the isochrones used are from the solar metallicity models of BCAH98, shown in Fig. 6. According to this model, the PMS stars commenced formation at the same time as the massive stars and ceased abruptly about 1 Myr ago.

chrones,[4] with mixing length parameter (l/H_p) of 1.9 at and above 0.7 $M_\odot$ and 1.0 below. In each case, we constructed the displayed isochrones by interpolating the tabulated data to find the specific ages we wished. We then transformed the L, $T_{\rm eff}$ data into the CMD plane using main-sequence Cousins colors, main-sequence bolometric corrections (Kenyon & Hartmann 1995), and the adopted λ Ori distance of 400 pc. We reddened the isochrones by the λ Ori value of $E_{B-V} = 0.12$. While this value may not be directly applicable to the stars in consideration, we note that the reddening vector for $R_V = 3.1$ is nearly parallel to the isochrones, so only a small age error would arise from a large reddening error. A steeper R_V value (e.g., 5.0, as measured in other parts of Orion) would cause the reddening vector to be even more closely parallel to the isochrones.

Comparison with these isochrones shows that indeed our newly discovered PMS stars are young, with most having ages of less than 3 or 10 Myr, depending on the model. We show in Figures 7 and 8 plots of the *star formation rate* versus time based on the DM98 and BCAH98 models, respectively. In each case, the rate is computed simply by counting stars between isochrones and dividing by the width of each age bin, while the error bars are the square root of the number of stars before the division. As seen from the figures, there is a striking difference in the age scale of these two results. The DM98 ages indicate a sharp onset of star formation about 3 Myr ago, with a peak in the range of 0.5–2 Myr ago. The star formation history computed instead with the BCAH98 model shows a peak at 2–3 Myr, with a more gradual onset about 5–7 Myr ago. The ages calculated with this model also exhibit a low age cutoff at 1 Myr. Although the model isochrones do cease at 1 Myr, the sharp truncation at this age is physical, as seen by the absence of stars above this isochrone in Figure 6. Note that the data in these figures reflect only a limited mass range and have not yet been corrected for incompleteness.

Evidently conclusions regarding the star formation history of the region will be dependent upon choice of stellar evolutionary model. We note that we have also considered other flavors of models from DM98 and BCAH98, which vary parameters such as abundances and convection parameters, as well as models from Swenson et al. (1994) and D'Antona & Mazzitelli (1994). The differences between models within each set are smaller than the differences between the sets. Therefore, for this paper we have chosen to do our analyses with the two models described above as representative of the range of model dependence. We will consider two evolutionary scenarios in § 5.

We further caution that a potential source of systematic error in the study of age distributions has been identified by D'Antona & Mazzitelli (1997). They have pointed out that higher mass stars progress along evolutionary tracks more quickly than lower mass stars, resulting in more closely spaced isochrones. Thus, an error in the mass scale of a set of tracks can change the relative age spread. Because, as detailed below, the BCAH98 tracks are systematically more massive than the DM98 tracks for the same star, we are not surprised that the latter produces a narrower spread.

In addition to the systematic differences between the stellar evolutionary models, there are other sources of uncertainty in our age determinations. First, our measurement error in $R-I$ color of 0.06 mag is not entirely negligible compared with the observed dispersion in color of roughly 0.13 mag. As such, it cannot be excluded that those stars found to have the oldest and youngest ages are extrema of the error distribution. However, photometric error can only account for a small portion of the observed age spread.

Second, the morphologies of the evolutionary tracks are such that our imposed magnitude cutoff of $R = 16$ does not

[4] We have used a version of these tracks with an extension to younger ages (1 Myr) and higher masses (1.2 $M_\odot$), courtesy of the Lyon Group.

permit complete detection of the lowest mass stars in our sample to ages as old as our goal of 30 Myr. Because the mass function most heavily weights the lowest mass stars, this could bias the age distribution of our sample to younger ages. Our upper magnitude cutoff (at $R = 12$) creates a similar, but less significant, bias for the youngest, most massive stars. In Figure 9 we show the distribution of ages for a sample of stars that we believe are unbiased by these effects. To create this sample, we examined the mass tracks for each model to identify the mass and age domains that are complete. For the DM98 model, we find that we are unbiased to stars between 0.3 and 10 Myr old for masses between 0.4 and 0.9 $M_\odot$. Similarly, for the BCAH98 model, we select stars between 1 and 10 Myr old with masses in the range of 0.5 to 1.2 $M_\odot$. We plot histograms of these subsamples in Figure 9. We find that the distributions shown in this figure are not statistically distinguishable from the distributions based on the full sample, despite the apparent morphological differences.

Finally, recent studies of PMS stellar populations have revealed that the PMS binary frequency is at least as high as that found in the field and is in some cases as much as a factor of 2 higher (for a review see Mathieu et al. 1999). Because of the luminosity enhancement of the system, undetected binaries in a sample of stars can cause one to overestimate the stellar luminosity and thus underestimate the age (see Simon, Ghez, & Leinert 1993). In fact, it is apparent from Figures 5 and 6 that our three double-lined stars appear to be near the top of the luminosity distribution for their colors. Thus, the mean age of stars implied by Figures 7 and 8 may be an underestimate for the system. However, the envelope of the oldest-appearing stars, which defines the turn-on time for star formation, likely represent single stars that are not affected by this bias, so the turn-on time interpretation should be valid.

An essential conclusion of these age analyses is that low-mass star formation did not begin prior to high-mass star formation in the λ Ori region. All of the newly discovered low-mass stars have ages consistent with formation within the past 5–7 Myr. This result is independent of both choice of stellar evolution models and systematic uncertainties. However, the detailed star formation history *is* model dependent and will be further discussed in § 5.

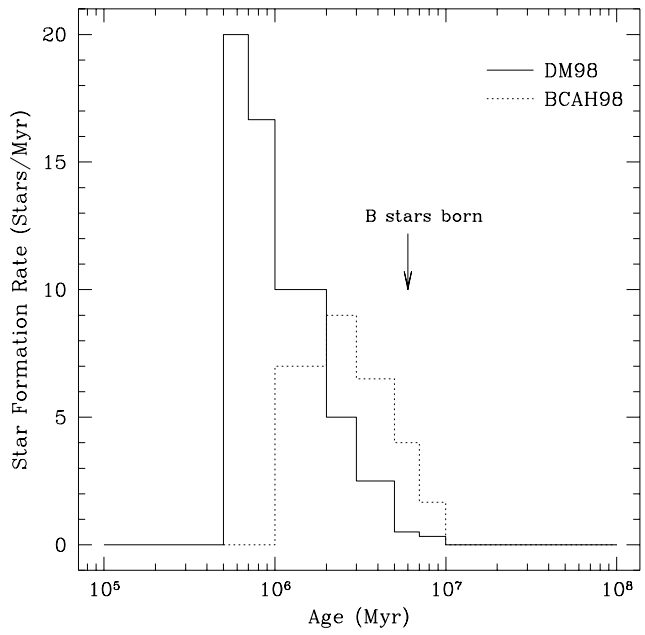

FIG. 9.—Data from Figs. 7 and 8 excluding stars of masses for which we have incomplete age coverage due to our magnitude limits.

3.3. *Completeness and the Mass Function*

One goal of this study is to investigate the IMF in the immediate vicinity of the OB stars, which we hereafter call the "local IMF," in contrast to the IMF of the entire star-forming region, which we call the "global IMF." Implicit in this definition of the local IMF is that the OB stars have always been closely associated spatially.

The completeness of our survey for low-mass stars is set by the completeness of our photometric survey, which defined the sample for spectroscopic observation, and by the completeness of the spectroscopic observations. Our photometric completeness is set partially by the USNO database, on which we have relied for stellar identification. The USNO study does not detect objects close to bright stars (i.e., those saturated on the POSS plates). Because we chose our field of interest to be close to the 11 OB stars, there are several small regions, most notably a hole around λ Ori, where we have no stars. However, our primary incompleteness derives from defects in the engineering-grade CCD chips of the Mosaic imager from which we derived our photometry. These defects have caused us to underestimate the brightness of as many as 15% of the stars by more than 0.4 mag. This certainly has caused us to falsely exclude some candidate PMS stars while falsely including very few. On the other hand, our spectroscopic completeness is quite good. We have observed 530 of 559 stars (95%) satisfying our photometric criteria (as well as 7 of 24 (29%) in our faint [$16 < R < 16.5$] addendum).

In total, we estimate that we have detected 75%–80% of the stars with strong lithium absorption in our magnitude range and within 7 pc in projection of the center of the OB stars. This incompleteness should be unbiased with respect to lithium absorption.

Our new observations focus on the lower end of the IMF. Specifically, the magnitude range of $12 < R < 16$ includes stars in a mass range of roughly $1.0\ M_\odot > M > 0.2\ M_\odot$, according to the DM98 models. However, because of our strict magnitude criteria, some of these masses are biased against particular ages. For example, a 0.3 $M_\odot$, 10 Myr star falls at $R = 17$ according to DM98 and thus cannot be detected in this survey. To avoid such age biases, we limit our analysis below to only those masses for which the ages of interest fall within our magnitude limits, where we are interested in ages between roughly 1 and 10 Myr. Thus, in the following computations we only consider stars with $0.9\ M_\odot > M > 0.4\ M_\odot$ for DM98 and $1.2\ M_\odot > M > 0.5\ M_\odot$ for BCAH98. These samples correspond to 31 and 42 stars, respectively.

In the following, we will compare the DM98 masses to those expected from field star IMF models. We will follow this analysis with presentation of comparable results for the BCAH98 masses.

Adopting a completeness value of 80% to correct the number of PMS stars in our sample, we may compare the local ratio of low- to high-mass stars to that predicted by the field IMF derived by Miller & Scalo (1979; assuming constant star formation and a Galactic age of 12 Gyr). Adjusting for our incompleteness, we estimate that there are

39 PMS stars in our field, given the mass range stated above.

If these stars derive from a fieldlike IMF, then the Miller & Scalo (1979) model predicts that we should see five stars with $M > 3\ M_{\odot}$, which corresponds to spectral type B9 or earlier. Instead, we see 11 such stars. Viewed the other way, given these 11 stars, one would expect to find 83 stars in the low-mass range if the Miller-Scalo model were valid for these stars. Thus, our completeness-corrected sample is deficient from the field by a factor of about 2.

To assess the significance of this difference between our sample and the field, we used a Monte Carlo algorithm (suggested by M. Meyer 1998, private communication) to compute the likelihood of arriving at our observed numbers. In each iteration of this algorithm, we select random masses from a log-Gaussian with Miller & Scalo (1979) parameters. We continue selecting until we have 50 (i.e. 11 + 39) stars in the high- and low-mass ranges specified above. After 100,000 iterations, we found that 2.6% of the test distributions had 11 or more massive stars. This indicated that our observed distribution differed from the field IMF with 97.4% confidence, in the sense that there are too few low-mass stars.

Considering the BCAH98 masses, the incompleteness-corrected 53 low-mass stars predict eight OB stars. The same Monte Carlo test as above predicts that this is different from the field IMF with only 81% confidence.

In summary, our observations suggest that the present-day local mass function differs from the field IMF with weak confidence. Whether this result implies that the local IMF also differs at all from the field will depend on to what extent the motions of the young stars have changed the mass function within the 7 pc radius around the OB stars that we have observed.

3.4. *Spatial Distribution of the PMS Stars*

In this study, we have chosen to look for PMS stars projected in the vicinity of the OB stars (Fig. 14 shows their spatial distribution). The question remains as to whether the stars we have found are part of a more distributed population independent of λ Ori or whether the PMS stars are indeed concentrated near their massive neighbors. To answer this question, we have performed a series of statistical tests on the spatial distribution of our sample.

As a control sample, we used the stars that we observed spectroscopically but that do not have detectable lithium by a conservative estimate (372 stars). We expect that this sample suffers the same spatial selection effects as our PMS sample but does not share the physical association of the latter sample. Thus, we expect that this control sample is derived from a uniform distribution.

We compared the spatial distribution of our PMS sample (72 stars) to the control sample using a Kolmogorov-Smirnov (K-S) test. We used the separation of each star from λ Ori as our independent parameter. The cumulative histograms of these two distributions are shown in Figure 10. Although the PMS sample shows a slight central concentration, the test reported that they were not significantly different from a uniform distribution (10% probability that they come from the same parent distribution). Thus, we have not detected any central concentration among the PMS stars.

Is it possible that the PMS stars did form in a centrally concentrated clump but in the stellar lifetimes of roughly

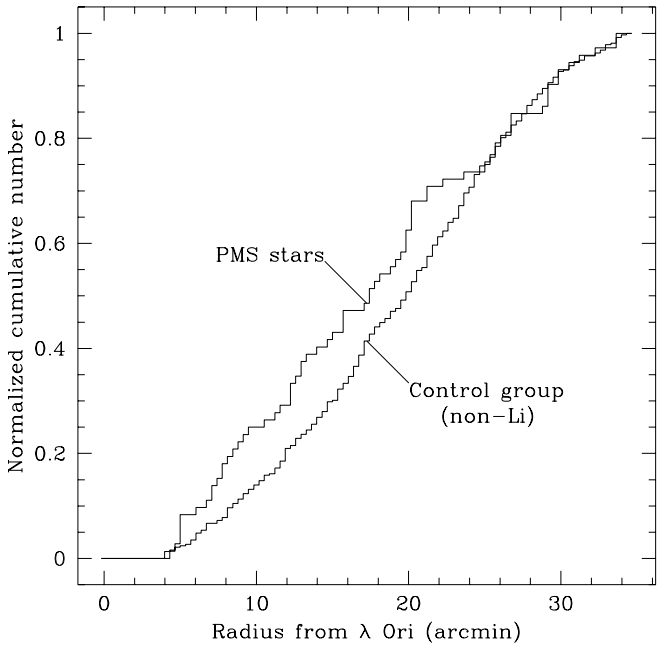

FIG. 10.—Normalized, cumulative distributions of stars in our WIYN spectroscopic sample as a function of radius from λ Ori. The upper distribution represents the PMS stars with strong lithium. The lower distribution is composed of stars with no detectable lithium. Stars with weak lithium or marginal detections are not included in either histogram. The flat part of the histograms at the left is due to λ Ori saturation on the POSS plates preventing detection of any faint stars nearby.

1–2 Myr the system has expanded to fill our field of view, thus washing out any spatial structure? To answer this question, we constructed a simple model of an unbound cluster of stars with three-dimensional Gaussian velocity and spatial distributions. We set the one-dimensional velocity dispersion to be 2.5 km s^{-1}, similar to our observed radial-velocity distribution. We then varied the initial cluster size (i.e., the σ of the spatial Gaussian distribution) and let the stars expand over time, ignoring gravity. As the distribution expanded, we noted the time at which a sample of stars with similar size to that observed here was no longer distinguishable from a uniform distribution.

We found that however concentrated was the initial cluster, it would not be identifiable as being centrally concentrated beyond 1.1 Myr. After only 0.75 Myr, a distribution of stars with an initial spatial dispersion greater than 2 pc would not be found to be centrally concentrated. In both of these cases, by the time the spatial distribution was indistinguishable from uniform, the model predicts that at least 50% of the stars would have escaped our 1° diameter field of view.

Thus, we note that our observed mass function (§ 3.3) may substantially undercount the low-mass stars born in the region observed, perhaps by enough to explain the observed deficiency in low-mass stars compared with the field IMF. However, if formed cospatially with the low-mass stars, the massive stars might undergo a similar expansion, thus leading to a similar undercounting. We discuss the spatial distribution of the OB stars below.

3.5. Hα *Measurements*

Why did we detect so many young stars where previous surveys found few? In particular, why did the DIL82 Hα survey find only two of the PMS stars in our field of study?

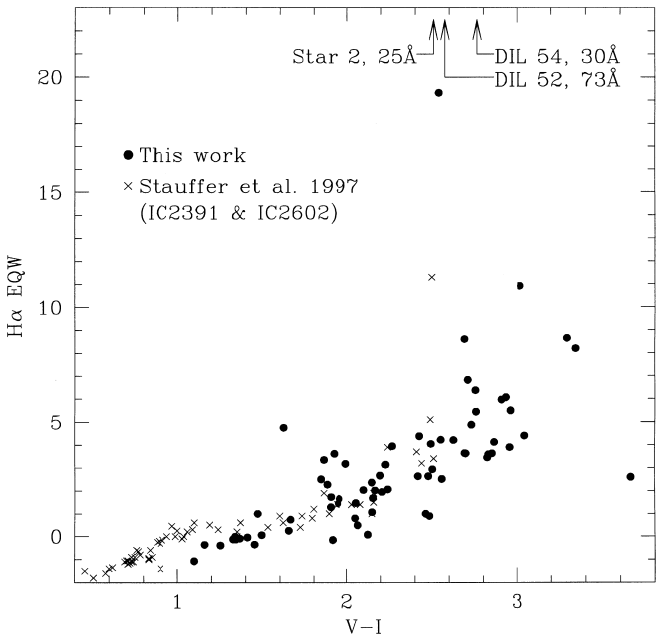

FIG. 11.—Comparison of Hα emission among λ Ori low-mass stars with ZAMS chromospheric Hα emission. The dots are λ Ori PMS stars, with three strong emission stars marked by arrows off the top of the figure. The W_λ(Hα) values of these three are indicated after their identifiers. The crosses are IC 2391 and IC 2602 stars from Stauffer et al. (1997). The similarity between these 30 Myr old stars and our PMS stars below about 12 Å demonstrates that most of our sample is comprised of chromospherically active WTTS.

To answer this, we examined the Hα lines of all our strong-lithium stars. We plot the equivalent widths of these lines versus $V-I$ in Figure 11. Subtraction of the spatially variable nebular Hα was the greatest contribution to the error in our measurements, which we estimate to be typically 1.0 Å. DIL 52 and DIL 54 (marked "very strong" and "very weak" emission sources, respectively, in the DIL82 survey) were the strongest Hα sources in our sample, at 73 and 30 Å, respectively. Our two stars with equivalent widths ∼20 Å were not detected by DIL82. Apparently, the equivalent width detection threshold for the DIL82 survey was about 25 Å for stars of similar magnitude to those in our survey.

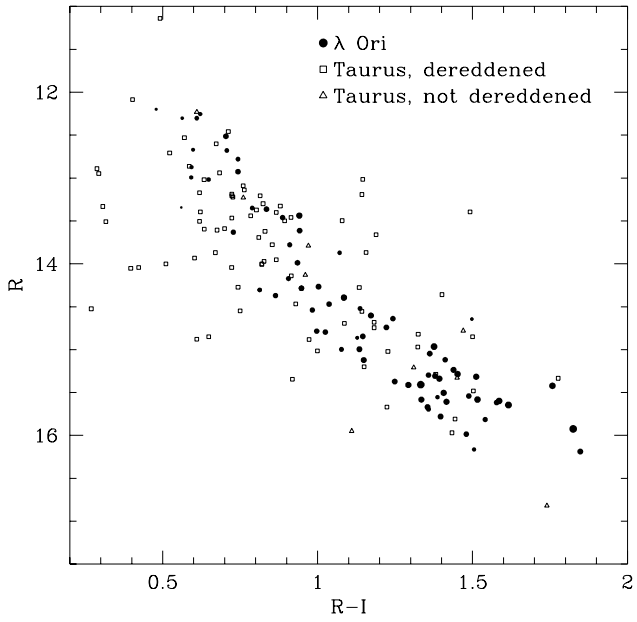

FIG. 12.—Comparison of λ Ori PMS stars to those in the Taurus-Auriga star-forming region (Kenyon & Hartmann 1995). This demonstrates, independent of any evolution model, that the λ Ori stars have similar ages to Taurus. The λ Ori dot size is proportional to W_λ(Li). The Taurus stars have been shifted by a distance modulus of 2.25 and have been dereddened where published A_V values are available.

Aside from these four stars with $W_\lambda(\mathrm{H}\alpha) > 12$ Å, our PMS stars have emission strengths typical of chromospheric activity. This linear distribution of Hα with increasing color bears a strong resemblance to the W_λ(Hα) versus $V-I$ distribution of the 30 Myr old clusters IC 2391 and IC 2602 (Stauffer et al. 1997). Thus, most of our PMS stars are WTTSs.

This result is in strong contrast to that found for the well-studied Taurus-Auriga star-forming region, for example. In that region, about half of the discovered PMS stars have strong Hα emission (as summarized in Kenyon & Hartmann 1995). We compare the Taurus stars to our sample in an R versus $R-I$ CMD in Figure 12, where we have shifted the Taurus literature photometry to the λ Ori distance. This figure permits a model-independent comparison of the PMS stars from this paper to the Taurus stars to demonstrate that they all have comparable ages. Given this result, the dearth of Hα in our sample is striking.

4. THE HIGH-MASS STARS

In this paper we have adopted global parameters of the λ Ori star-forming region from the literature. In particular, we have assumed 11 OB stars at an age of 2–6 Myr and a distance of 400 ± 40 pc, all from MP77. In this section, we will examine each of these parameters.

4.1. *The OB Population*

Within the region of our survey, the MP77 sample includes one O8 III star (λ Ori), three B0–B2 stars and seven B8–B9 stars. The MP77 sample came primarily from the Henry Draper Extension (HDE) catalog selected for stars in the center of the association. Thus, as a sample of the massive stellar component of the entire λ Ori star-forming region, it is incomplete spatially and perhaps photometrically because of the HDE catalog magnitude limits.

To test whether there may be more OB stars in the λ Ori region, we searched the *Hipparcos* Input Catalog (HIC; ESA 1997) and the Positions and Proper Motions Catalog (PPM; Roeser & Bastian 1988) for any stars on or inside the molecular ring with OB spectral types. Of the 11 OB stars identified by MP77 in the 1° field around λ Ori, we found five in HIC and nine in PPM. Neither of these catalogs included OB stars in the central 1° field that were not identified by MP77. Outside this field, but within a 4° radius of λ Ori defined roughly by the CO ring, HIC identifies an additional 15 B stars, while PPM includes 29. We note that the overlap is complete: every HIC star enumerated here was also found in the PPM catalog. Neither of these catalogs identify any O stars other than λ Ori in this region.

Presuming that the PPM is not spatially biased within the domain of the λ Ori star-forming region, we examined the spatial distribution of all the OB stars found in these two surveys as a function of radius from λ Ori with an outer limit of 4°. A K-S test demonstrated that the distribution of PPM OB stars is significantly different (0.5%) from a uniform distribution in the sense of being centrally concentrated. Thus, we conclude that the apparent central concen-

tration of massive stars is real and that most of the 11 OB stars identified by MP77 are likely members. Little more can be said about the entire OB population of the star-forming region until a more detailed study of all candidate massive stars is completed.

4.2. *Distance*

MP77 measured the distance to the star-forming region by a main-sequence fit of the B stars in the field center, yielding a distance modulus of 400 ± 40 pc. For the five stars that the *Hipparcos* catalog has in common with MP77, we can compare the measured geometric parallax distances to the main-sequence fit distance. We find that these distance measurements are consistent, but at 400 pc, the *Hipparcos* parallaxes have rather large errors (about 30% fractional error). Thus, we cannot improve on the MP77 calculation by this means. We will continue to assume a distance of 400 pc, noting that this distance is comparable to those found for other star-forming regions in the Orion molecular cloud complex.

4.3. *Ages*

The age of the OB stars calculated by MP77 is in the range of 2–6 Myr, depending on which stars are considered. The 6 Myr age comes from identifying a main-sequence turnoff at B0. The younger end of the age range comes from a 2–3 Myr estimate for λ Ori itself, an O8 III star.

A dynamical age estimate for the dispersal of the molecular cloud can also be computed from the models of the expansion of the molecular ring in conjunction with cloud radial-velocity measurements. MM87 calculate that constant-velocity expansion of the ring corresponds to an age of 2.4 ± 0.4 Myr. Lang & Masheder (1998) find a higher expansion velocity using higher quality data than MM87, leading to a constant-velocity expansion time of 1.8 Myr. If instead the ring expansion has been accelerated by the OB stars, MM87 compute an age of 5.9 Myr.

We note that the connection between the evolutionary age of the OB stars and the dynamical age of the molecular ring may not be straightforward. We discuss this further in § 5.

4.4. *Kinematics*

The *Hipparcos* data complicate our understanding of the OB star system. High-precision proper-motion measurements exist for five of the 11 OB stars. These data indicate that the OB stars are moving rapidly, with tangential velocities of about 5 km s^{-1} at a distance of 400 pc. Using these measurements, we have extrapolated linearly back in time. Figure 13 shows the current locations of these five stars and their projected locations 3 Myr ago. The error bars correspond to the proper-motion errors.

This figure presents two surprising results. First, if their dynamical age is as great as the MP77 evolutionary age, then the current trajectories imply that they were born near or beyond the present-day ionization front. Second, the proper-motion trajectories suggest that the OB stars have been converging on the center of the field over time, only to achieve a tight cluster at the present day. If we are to believe the proper motions are indicative of past motion, then we are observing the massive stars at a special time when they have arrived at their minimum distance from each other.

We consider both of these implications to be implausible. Instead, we infer that the expansion age of the massive-star system is smaller than their evolutionary age. That is, the present trajectories of the OB stars are not representative of their kinematic history. We argue later that they may have recently been unbound from a dense parent cloud. If so, their present velocity dispersion should reflect the velocity dispersion of that cloud. Correcting for *Hipparcos* measurement error, we compute a two-dimensional dispersion of 3.5 km s^{-1} for the five OB stars in Figure 13. This is equivalent to the one-dimensional velocity dispersion of 2.6 km s^{-1} found among the low-mass stars and is comparable to those of molecular clouds. If we exclude the proper-motion outlier, HD 36822, we instead find a two-dimensional dispersion of 1.8 km s^{-1} but with a group motion heading southward at 5.1 km s^{-1}.

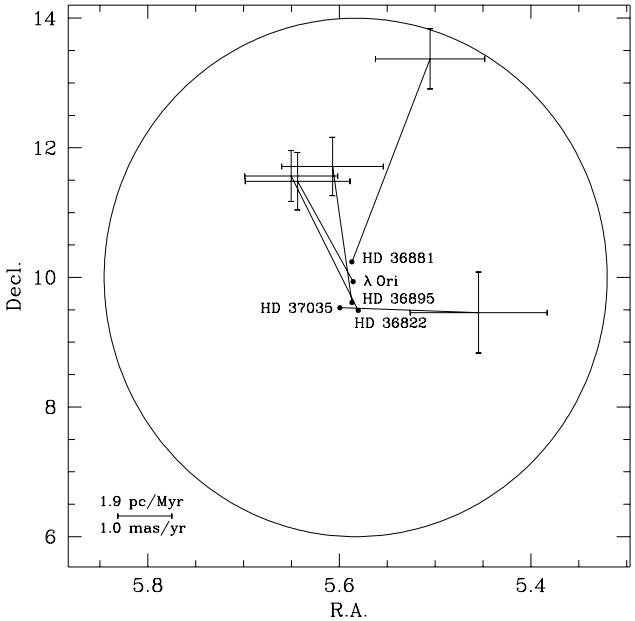

FIG. 13.—Positions of 5 OB stars 3 Myr ago, based on *Hipparcos* proper-motion data. The error bars indicate proper-motion errors. The circle schematically indicates the position of the ionization front at the present epoch.

Another intriguing datum is the radial velocity of λ Ori. Velocity monitoring by R. D. Mathieu & J. A. Morse (1999, private communication) suggests that this star is a binary with a system velocity ($V_{LSR} \sim 18$ km s^{-1}) as much as 6–8 km s^{-1} redward of the B30/35 clouds and our PMS stars. Thus, if λ Ori is at the star-forming region center now, it will not be there for long.

4.5. *Summary*

The interpretation of the OB star system is more complicated than has been considered in previous studies. Although the OB concentration highlighted by MP77 appears to be real, there are many other less-studied B stars in the region. Furthermore, the kinematics of a subset of the central stars demonstrate that the dynamical age of the star-forming region may be significantly younger than the OB evolutionary ages. We postulate that these stars became unbound from their parent cloud as recently as a million years ago.

5. DISCUSSION

We have spectroscopically surveyed a 1° field at the center of the λ Ori star-forming region to search for young low-mass stars. Our most significant result is that we have found 72 low-mass PMS stars in a field that has been pre-

viously thought to be dominated by OB stars (see Fig. 14). Classical survey techniques (Hα, X-ray) had found only two PMS stars.

Our discovery raises the following issues for understanding the star formation history of this region.

1. Comparison of the ages of the PMS stars to turnoff evolutionary ages for the OB stars suggests that the vast majority of PMS stars are coeval with or younger than their massive counterparts with ages of 2–6 Myr. In more detail, comparison with the DM98 models suggests that the low-mass star formation occurred after the formation of the OB stars. Comparison with the BCAH98 models indicates that the formation of both high- and low-mass stars began concurrently and that the formation process was abruptly terminated roughly 1 Myr ago.
2. The age spread of the PMS stars in the context of DM98 models is too narrow for subsonic synchronization in a cold cloud. To coordinate the births to within a few Myr, one needs a shock or an ionized medium.
3. The massive star kinematics suggest that the OB star system has not been freely expanding for more than 1–2 Myr.
4. We detect no central concentration of the PMS stars within the 3.5 pc projected radius of this study.
5. Although the observed mass function in the vicinity of the OB stars is marginally deficient in low-mass stars compared with the field IMF, kinematic models suggest that a substantial fraction of the stars formed in the region may have already dispersed. Thus, the true mass function could easily match or even exceed the field for relative numbers of low-mass stars.
6. There is a marked lack of T Tauri–like Hα emission in the PMS sample, despite their youth.

In the following sections, we present two scenarios for the evolution of the star-forming region that explain the above features. As we did for the analyses in § 3, we discuss two distinct evolutionary models based on the age distributions derived from two sets of stellar evolutionary models.

5.1. *Coeval Star Formation: The BCAH98 Results*

Figure 9 shows us that in the context of the BCAH98 stellar evolution models, the PMS stars began to form about 5–7 Myr ago. The formation rate peaked at 2–3 Myr and subsequently dropped to near zero in the past million years. These age estimates resonate with the ages calculated for the OB stars: most of the B stars formed 6 ± 1 Myr ago, while λ Ori is 2–3 Myr old (MP77). Thus, with these evolutionary tracks we conclude that the birth of the majority of

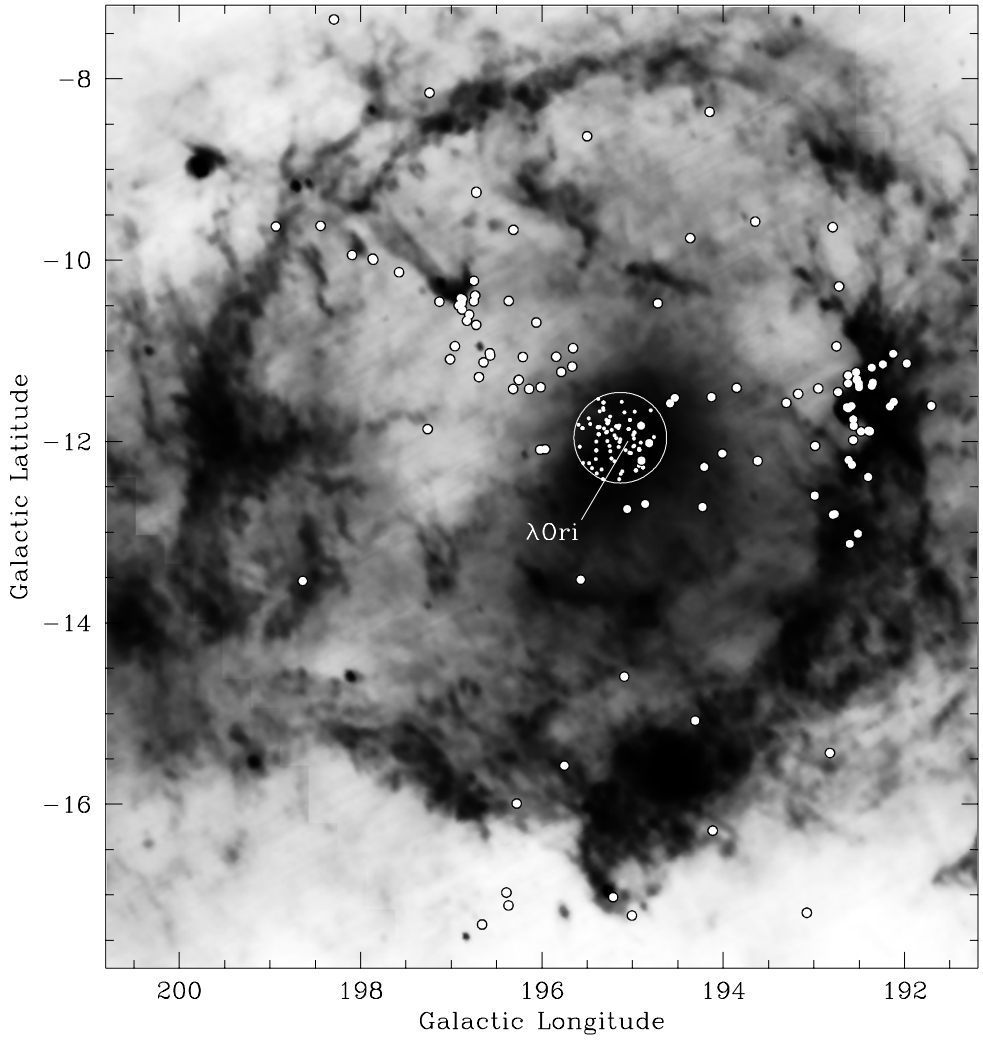

FIG. 14.—Contrast of our detection efficiency to previous work. Our spectroscopic survey for lithium has revealed a much higher density of young stars (*small dots*; 72 stars in 0.75 deg^2) than previous Hα and X-ray surveys (*large dots*; 108 stars in 100 deg^2). The background gray scale is an IRAS 60 μm image courtesy of SkyView (McGlynn et al. 1998) on the same scale as in Fig. 1.

the massive stars coincided with the beginning of low-mass star formation. That is, the conditions in the parent molecular cloud about 6 Myr ago were appropriate for both high- and low-mass star birth.

This model also tells us that the star formation was terminated rapidly 1 Myr ago. Significantly, the timing of this event corresponds roughly with the time for the breakup of the parent cloud, which we derived from consideration of the OB star kinematics in § 4.4.

These two results lead us to the conclusion that until recently star formation was an ongoing activity in a massive, gravitationally bound molecular cloud core. The cloud not only continued to issue PMS stars but also maintained enough mass to bind the newly formed stars to itself. Then, roughly 1 Myr ago, the cloud was dispersed, halting star formation and releasing the stars into nearly free expansion.

We note that this scenario implies that the stars were in a higher stellar-density environment at the time of their release. As such, we will suggest below that the lack of evident disks (identified by strong Hα emission) may result from prolonged exposure to the luminous OB stars. The present lack of central concentration within our 7 pc–diameter field of both the OB stars and the low-mass stars results from expansion and also implies that some stars from the original cluster are likely present outside the boundaries of our field of view. This may account for the presently observed deficiency of low-mass stars compared to the field IMF, particularly if the OB stars were initially more centrally concentrated (as in the Trapezium cluster).

What could have caused this cloud to break up? We see very little evidence of dense gas at the center of the star-forming region today (see Fig. 1), so the dispersal process must have been quite efficient. Below, we will consider the possibility that a supernova may have triggered this event.

5.2. *A Burst of Star Formation: The DM98 Results*

In the context of the ages inferred from the DM98 models, we arrive at a rather different picture of the evolutionary history of the region. In this scenario, the formation of low-mass PMS stars began recently, about 2–3 Myr ago. The DM98 models suggest that very few low-mass stars formed coevally with the B stars but that the low-mass birthrate increased dramatically around the time that λ Ori was formed. The coincidence of onset with the age of λ Ori motivates consideration of λ Ori (and in particular the ionization front which it has driven) as a trigger for low-mass star formation.

Additionally, the narrow age spread of the PMS stars may be evidence of triggered star formation. As seen in Figure 9, the width of the age distribution is very small for the DM98 model: on the order of 1 Myr. To synchronize such a burst of star formation over the entire 7 pc–diameter field, a communication velocity of at least 3 km s^{-1} is necessary. However, the typical sound speed in a cold, molecular cloud is only a few tenths km s^{-1}. To achieve this synchronization at subsonic speeds would require an initial parent cloud with a radius of less than 1 pc. Even given kinematic expansion, such a central concentration of the low-mass star formation should still be observable 1 Myr later but is not seen (§ 3.4).

The implication is that we require an external trigger for the formation of low-mass stars. Natural candidates are the winds and/or ionizing flux from λ Ori and its massive neighbors. However, we have found some PMS stars that are much younger than λ Ori. How can we have stars forming as recently as 0.5 Myr ago when λ Ori should have ionized all of the nearby gas after its birth 2–3 Myr ago? We consider here two plausible explanations: (1) many of the observed PMS stars were not born in close proximity to the OB stars, or (2) λ Ori did not immediately disperse the nearby molecular gas and instead the gas was dispersed recently by a supernova. We discuss the former explanation here and the latter (preferred) explanation in a separate section below.

Given that we see no central concentration of the low-mass stars within our field of view, it is possible that the stars that we have observed are part of a larger system that is not immediately cospatial with λ Ori but rather is more distributed both along and across our line of sight. In this scenario, we envision an ionization front expanding outward from λ Ori, causing compressional formation of stars as it passes. Thus, the stars first formed would be closest to λ Ori, while the youngest stars would be nearest the present position of the ionization front.

While not obviously contradicted by any information in hand, this scenario does suffer from an inability to explain several essential observations. First, if the 2–3 Myr ages of λ Ori and the oldest low-mass stars are correct, it is not evident how the clustering of the OB stars maintained itself over this period of time. This is ample time for the OB stars to move apart, given their measured proper motions. Second, there is no obvious reason why stars formed in this way should lack disks and Hα emission. In the model in consideration, many (and especially the youngest) PMS stars are far removed from λ Ori, and it seems unlikely that the ionization front itself could both cause molecular cores to form stars and disperse subsequently formed disks. Finally, given that many stars were formed within the last million years, the lack of substantial molecular gas along the line of sight in our field of view is a concern.

5.3. *The Supernova Hypothesis*

The possibility of a supernova in the vicinity of λ Ori has been considered by several authors (see Cunha & Smith 1996 and references therein) to explain the molecular ring and λ Ori's peculiar motions. A recent supernova would also play a key role *either* as a trigger for the birth of the low-mass population near the OB stars (DM98) or as the gas dispersal mechanism that terminated low-mass star formation (BCAH98).

We hypothesize that a supernova progenitor was born with the B stars about 6 Myr ago in a massive molecular cloud, perhaps in the core of the giant molecular cloud suggested by DIL82. After a presupernova lifetime of 5 Myr (corresponding to about a 30 $M_\odot$ star according to Schaller et al. 1992), the star exploded about 1 Myr ago, disrupting the parent cloud.[5] After breaking out of the cloud, the blast expanded to create a giant H II region, which is maintained by λ Ori and its massive companions today.

This scenario is appealing for both the ongoing and burst star formation pictures discussed above. In both cases, gravitationally binding the OB stars with the parent cloud for much of their lifetime solves the paradox of their contin-

[5] Perhaps, as suggested by MM87, the λ Ori binary was bound to the SN progenitor, explaining λ Ori's unusual radial velocity but requiring a revision of the 2–3 Myr age of λ Ori.

ued spatial association despite large velocities. As already mentioned, in the ongoing star formation scenario, the supernova provides a natural explanation for the cessation of stellar birth 1 Myr ago. In the burst scenario, the supernova itself triggers the formation of low-mass stars. Thus, it explains naturally the differences in the ages of the high- and low-mass stars and the narrow age spread of the low-mass stars. There remains, however, the question of how star formation could continue essentially until the present day. We note though that if the supernova occurred roughly 1 Myr ago, ambiguities in the zero points of the evolutionary tracks begin to become a significant fraction of the stellar lifetimes (Hillenbrand 1997). The possibility that all of the stars are more coeval than the DM98 ages suggest should be carefully considered.

A critical issue for this supernova conjecture is whether a massive parent cloud can survive the formation of a massive star for the presupernova lifetime of the star. O stars are thought to typically reside confined in their parent cores as ultracompact H II regions for only 10%–20% of their main-sequence lifetimes (Wood & Churchwell 1989).

More generally, a significant concern is our reliance on the published OB ages of MP77. Certainly, models of post–main-sequence evolution of massive stars have improved since that investigation. More importantly, we suspect that higher quality analyses can be made with narrowband photometry, and we have embarked on obtaining Stromgren photometry for this purpose.

Finally, we note that the age difference between the OB and low-mass stars that we find here has precedents. Hillenbrand (1997) finds very much the same results in the Orion Nebula Cluster, as do Walter et al. (1994) in the Sco-Cen association. This indicates that the formation history of the λ Ori region may resemble other regions. However, Preibisch & Zinnecker (1999) found agreement in age between the high- and low-mass stars in Upper Sco. We note that there may be systematic errors between very different methods of determining high-mass and low-mass stellar ages. We are sorely in need of a careful calibration of stellar ages across all stellar masses for ages less than 1 Myr.

5.4. *Missing Accretion Diagnostics*

Despite their apparent youth, most (all but four) of our PMS stars are lacking in T Tauri–like Hα emission. Instead, the weak emission we observe is typical of chromospheric activity. Since T Tauri Hα emission is typically taken as a diagnostic of disk accretion, we find that 93% of our PMS stars show no sign of disk activity. Is it possible that these stars have already lost their disks? Could the OB stars have disrupted the circumstellar environment of the PMS stars?

In Trapezium models, Johnstone, Hollenbach, & Bally (1998) find that far-UV flux from θ^1C Ori (an O6 star) can photodissociate the outer layers of circumstellar disks from a distance of 0.3 pc. Inside this distance, disks are observed to have mass-loss rates on the order of $10^{-7}\ M_\odot\ \mathrm{yr}^{-1}$. The λ Ori OB association has a similar number of massive stars to the Trapezium, but λ Ori is less luminous than θ^1C Ori. Thus, this mechanism seems unlikely to be able to destroy the outer disks of PMS stars as far as 3.5 pc away from λ Ori, even given a million years.

However, if the PMS stars were bound within their parent gas cloud for a million years or more, as implied by the group star formation scenario above, the orbits of these stars could have brought them close to one or more of the OB stars in their lifetime. Thus, we conjecture that the Hα signatures of our PMS stars may differ from regions like the Trapezium or Taurus because of the persistence of a massive parent cloud binding the high- and low-mass stars together in a small space. That is, Taurus may be too diffuse and Trapezium may be too young to show such disk depletion. This idea may not work for the burst scenario, though, as the young PMS ages and kinematic dispersal of stars likely does not allow enough of the low-mass stars to have an encounter with an OB star. Future surveys may use other disk diagnostics, e.g., IR excess, to answer whether the disks have in fact been disrupted.

5.5. *Mass Distribution*

One of the goals of our research program is to assess whether the *local IMF* in the immediate vicinity of OB stars is the same as either the *global IMF* of a giant molecular cloud or the IMF derived from field stars. Our interest was motivated by the fact that the DIL82 Hα survey had detected only two low-mass PMS stars among the OB stars, strongly suggesting that the formation of the OB stars had not been accompanied by cospatial formation of a low-mass population. Our discovery of 70 additional low-mass PMS stars has shown clearly that this first impression was wrong and resulted from the bias inherent in an Hα survey.

The question remains, however, how the local IMF compares to that of the entire star-forming region or the field. With this first report we cannot yet make a definitive statement. While our sample suggests that the number of low-mass stars among the OB stars is less than would be expected from a field-based IMF, the statistical significance of this distinction is marginal with these data. Furthermore, we consider it likely that kinematic expansion has removed some fraction of the low-mass population from our field of view.

Similarly, the global IMF is not yet well defined. There are 29 more B stars known in the 8°-diameter area encompassing the region, most of which are of later type (§ 4.1). But comparison with the density of late-B stars outside the star-forming region suggests that few and perhaps none are actually members of the association. In addition, they show a nearly uniform distribution on the sky, unlike the prominent central concentration of the MP77 B stars. Nonetheless, until examined these distributed B stars represent an important ambiguity in the high-mass end of the observed mass function. Another 107 low-mass PMS stars are already known elsewhere in the star-forming region as a result of X-ray and Hα surveys. Should only a few of the B-star candidates turn out to be association members, these PMS stars are already ample to make the global IMF consistent with the field IMF. Indeed, given that our technique has revealed many times more stars than either of these survey techniques, it is quite possible that the low-mass star population may exceed the expected number based on the field IMF. We have begun an extension of this work by increasing the spatial coverage by an order of magnitude, which should clarify the situation.

6. CONCLUSIONS

In a photometrically selected spectroscopic survey, we have identified 70 previously unknown (and two previously known) PMS stars within a 3.5 pc (projected) radius around the O8 III star λ Ori. Our survey technique relies on identi-

fication of strong lithium absorption lines in all candidate stars with PMS photometric properties and is sensitive to stars younger than about 30 Myr. With the advent of multi-object spectroscopy this technique is comprehensive, unbiased, and efficient in terms of total telescope time (11 hr on sky start to finish), as well as data reduction effort.

Interpretation of the star formation history of the region is dependent upon choice of stellar evolution models. All models considered show that very few low-mass stars formed before the OB stars. Evidently the environment did not promote formation of low-mass stars until the birth of the massive stars. Comparison with BCAH98 isochrones show that the high- and low-mass stars began to form at the same time and continued until an abrupt termination roughly 1 Myr ago. On the other hand, comparison with DM98 isochrones indicate that these stars are younger than the OB stars and have a small age spread indicative of a burst of star formation. This spread is too narrow to arise from subsonic processes in molecular gas and thus would be an indicator of triggered star formation.

Using *Hipparcos* data, we find that the proper motions of the OB stars are too high for them to remain spatially associated for more than 1 Myr. This evidence implies that the stars were gravitationally bound until quite recently, yet there is very little gas in their vicinity now. We conjecture that a supernova explosion in the midst of the parent molecular cloud 1 Myr ago can explain the OB kinematics, as well as the PMS ages. This event would release the binding mass of the dense gas. Additionally, it would cease stellar birth, as seen in context of the BCAH98 isochrones. Or the compressive effects of the expanding shock could trigger the collapse of portions of the cloud, creating the burst of formation implied by the DM98 isochrones.

Perhaps our most remarkable result is that only 5% of young PMS stars have strong Hα emission indicative of accretion disks. We conjecture that the radiation fields of the massive stars may have disrupted the circumstellar disks while the entire association was tightly bound within the parent molecular cloud. Future IR observations of the PMS stars will provide more direct evidence regarding the presence of disk material.

We would like to thank G. Jacoby, H. Bond, and F. Vrba for their generous assistance in obtaining photometry for this study. C. J. D. acknowledges support from the NASA National Space Grant College and Fellowship Program through the Wisconsin Space Grant Consortium, as well as a Grant-in-Aid-of-Research from Sigma Xi. This work is supported by NSF grant AST 94-1715.

REFERENCES

Alcalá, J. M., Terranegra, L., Wichmann, R., Chavarría-K. C., Krautter, J., Schmitt, J. H. M. M., Moreno-Corral, M. A., De Lara, E., & Wagner, R. M. 1996, A&AS, 119, 7
Baraffe, I., Chabrier, G., Allard, F., & Hauschildt, P. H. 1998, A&A, 337, 403 (BCAH98)
Briceño, C., Hartmann, L. W., Stauffer, J. R., Gagne, M., & Stern, R. A. 1997, AJ, 113, 740
Cunha, K., & Smith, V. V. 1996, A&A, 309, 892
D'Antona, F., & Mazzitelli, I. 1994, ApJS, 90, 467
———. 1997, Mem. Soc. Astron. Italiana, 68, 807
———. 1998, in ASP Conf. Ser. 134, Brown Dwarfs and Extrasolar Planets, ed. R. Rebolo, E. L. Martín, & M. R. Zapatero Osorio (San Francisco: ASP), 442
Diplas, A., & Savage, B. D. 1994, ApJS, 93, 211
Duerr, R., Imhoff, C. L., & Lada, C. J. 1982, ApJ, 261, 135 (DIL82)
ESA. 1997, The *Hipparcos* Catalog (ESA SP-1200)
Evans, D. S. 1967, in IAU Symp. 30, Determination of Radial Velocities and Their Applications, ed. A. H. Batten & J. F. Heard (London: Academic Press), 57
Gomez, M., & Lada, C. J. 1998, AJ, 115, 1524
Hillenbrand, L. A. 1997, AJ, 113, 1733
Johnstone, D., Hollenbach, D., & Bally, J. 1998, ApJ, 499, 758
Kenyon, S. J., & Hartmann, L. 1995, ApJS, 101, 117
Lang, W. J., & Masheder, M. R. W. 1998, Publ. Astron. Soc. Australia, 15, 70
Maddalena, R. J., & Morris, M. 1987, ApJ, 323, 179 (MM87)
Maddalena, R. J., Moscowitz, J., Thaddeus, P., & Morris, M. 1986, ApJ, 303, 375
Magazzù, A., Martín, E. L., Sterzik, M. F., Neuhaüser, R., Covino, E., & Alcalá, J. M. 1997, A&AS, 124, 449
Mathieu, R. D., Ghez, A. M., Jensen, E. L. N., & Simon, M. 1999, Protostars and Planets IV, in press
McGlynn, T., Scollick, K., & White, N. 1998, in IAU Symp. 179, New Horizons from Multi-Wavelength Sky Surveys, ed. B. J. McLean, D. A. Golombek, J. J. E. Hayes, H. E. Payne (Dordrecht: Kluwer), 465
Miller, G. E., & Scalo, J. M. 1979, ApJS, 41, 513
Monet, D., et al. 1996, USNO-A1.0, (Washington: USNO)
Murdin, P., & Penston, M. V. 1977, MNRAS, 181, 657 (MP77)
Neuhaüser, R., Torres, G., Sterzik, M. F., & Randich, S. 1997, A&A, 325, 647
Preibisch, T., & Zinnecker, H. 1999, AJ, 117, 2381
Roeser S., & Bastian, U. 1988, A&AS, 74, 449
Schaller, G., Schaerer, D., Meynet, G., & Maeder, A. 1992, A&AS, 96, 269
Simon, M., Ghez, A. M., & Leinert, C. 1993, ApJ, 408, L33
Stauffer, J. R., Hartmann, L. W., Prosser, C. F., Randich, S., Balachandran, S., Patten, B. M., Simon, T., & Giampapa, M. 1997, ApJ, 479, 776
Sterzik, M. F., Alcalá, J. M., Neuhaüser, R., & Schmitt, J. H. M. M. 1995, A&A, 297, 418
Swenson, F. J., Faulkner, J., Rogers, F. J., & Iglesias, C. A. 1994, ApJ, 425, 286
Walter, F. M., Vrba, F. J., Mathieu, R. D., Brown, A., & Myers, P. C. 1994, AJ, 107, 692
Wolk, S. J. 1996, Ph.D. thesis, State Univ. New York, Stony Brook
Wood, D. O. S., & Churchwell, E. 1989, ApJS, 69, 831